

# Field Emission Dark Current of Technical Metallic Electrodes

F. Le Pimpec\*, R. Ganter, R. Betemps

Paul Scherrer Institut  
5232 Villigen  
Switzerland

June 15, 2019

## Abstract

In the framework of the Low Emittance Gun (LEG) project, high gradient acceleration of a low emittance electron beam will be necessary. In order to achieve this acceleration, a -500 kV, 250 ns FWHM, pulse will be applied between two electrodes. Those electrodes should sustain the pulsed field without arcing, must not outgas and must not emit electrons. Ion back bombardment, and dark current will be damaging to the electron source as well as for the low emittance beam. Electrodes of commercially available OFE copper, aluminium, stainless steel, titanium and molybdenum were tested, following different procedures including plasma glow discharge cleaning.

\PACS 29.25.BX \sep 52.80.Vp \sep 79.70.+q

## 1 Introduction

In the framework of the Low Emittance Gun (LEG) project, an X-ray free-electron laser (FEL) based on a field emitting cathode is expected to deliver six orders of magnitude higher peak brightness than current state-of-the-art light sources, together with a thousand times shorter pulses [1, 2].

To rapidly accelerate the electrons emitted by the electron source, and keep the emittance low, a stable pulsed voltage in the megavolt range is needed. The first project phase is to design and test an ultra high vacuum (UHV) 500 kV pulser using a resonant air-core transformer (Tesla coil) [3]. A pulse of 250 ns (full width at half maximum), -500 kV, working at 10Hz, will be applied between the cathode holder and an extracting anode. During this time, electrode materials should sustain the field without arcing and the dark current should be kept as low as possible. This dark current will ionize the residual gas as well as desorbing neutrals and ions by the known electron stimulated desorption process (ESD) [4, 5]. Those ions will be accelerated toward the cathode and the field emitter array

---

\*Frederic.le.pimpec@psi.ch

(FEA), in other words the electron source, and induce sputtering. It is known that some surfaces are more sensitive than others to very low energy ion bombardment. Measurable damage can already occur at 500 eV [6, 7, 8]. The damage induced, from any kind of energetic ions, will then reduce the electron emission and the lifetime of the field emitter, for example in GaAs photocathodes, used as polarized electron sources for accelerators [9, 10]. During the after pulse, the reversed field will accelerate the ions toward the extracting anodes producing a current of electrons which will also back bombard the field emitter. The gas desorbed can induce a pressure rise which might not disappear before the next pulse. In the worst case, a plasma forms followed by breakdown and sputtering of the anode material to the field emitter cathode. Recent work, and thorough review of over a century of vacuum breakdown research in many areas, [11, 12, 13] is still not sufficient to select electrode materials without application specific testing.

In order to investigate the electrodes material, a DC high gradient test stand was built to test different metals, which were potentially suitable as electrodes in the pulser. The goal is to find the most suitable material, for our needs, which can sustain high field without breakdown, and emits almost no electrons. In situ cleaning by plasma glow discharge was also tested to see whether an improvement was noticeable in the mitigation of the dark current. This technique of gas conditioning to lower the field enhancement factor  $\beta$  has already been reported [14, 15, 16] and used successfully in accelerators to process niobium accelerating cavities, see description in [12], as well as for curing other issues [17].

## 2 System setup and electrode preparation

### 2.1 System setup

The ultra-high vacuum (UHV) system shown in Fig.1, outside its metal confinement bunker for radiological protection, is pumped by a 150 l/s diode ion pump. The average pressure reached is in the low  $10^{-9}$  Torr scale after a quick bake of the ion pump. A more thorough bake brings the pressure down to the mid  $10^{-10}$  Torr. An injection line, a leak valve and a Torr capacitance gauge allow the controlled injection of a chosen gas into the system to prepare the glow discharge between the electrodes. In order to clean the anode and the cathode at the same time, a third electrode polarized positively in respect to the test electrodes is used, Fig.2. The distance of this third electrode from the center of the chamber is a constant.

A negative and continuous 0 to 100 kV bias is applied to the cathode through an insulating ceramic, (on the left in Fig.1). The anode is grounded. The capacitance of the system is close to 300 pF, hence the potential energy stored is 1.5 J at 100 kV. The current flowing from the cathode to the anode is measured across a  $1 \text{ M}\Omega$  resistor with a digital Fluke<sup>TM</sup> voltmeter. The gap separation between the electrodes is adjustable via a translation feedthrough and is controlled with a mechanical comparator. The sagging due to the weight at the end of the rods means that the two electrodes are not centered on each other. We do not expect this off centering to be of any consequence to the high voltage processing. However, it explains the off center damages seen on cathodes. Accurate measurement of the current to the 50 pA level is achieved.

## 2.2 Electrode choice

Given the long history of research on vacuum breakdown, it seems that the choice of the electrodes should be easy. However, as there is no universal quantifying theory to explain the process of vacuum breakdown depending on the material, and its surface state (physical and chemical), it is necessary to do our own testing for our own application. In order to pick the most appropriate material, we study some elemental properties. Many tables of elements are then compiled in order to make an informed choice. In our case, the electrodes should sustain a DC pulse of 500 kV and not produce or have a low electron dark current. Also a FEA will be installed in the middle of the cathode. If any arcing occurs, sputtered, or vaporized, anode material will deposit on the FEA. This can lead to destruction of the FEA, and the necessity to exchange it; in our system this is a complex and time-consuming procedure. Table.1, compares the secondary electron yield (SEY) the sputtering rate, the melting point, and the tensile modulus of the candidate elements.

From Table.1, Cu and Au appear to be bad candidates. Results obtained with RF waveguide support this point [22]. Despite its good electronic and ionic properties Al should be discarded, as the combination of melting point and elastic modulus is low compared to other materials. Al will probably coat a FEA thoroughly in case of arcing, as we also found with a gold coated anode. The FEA coating problem further implies that spark processing to reach high gradient, despite being efficient, should be avoided [23, 24], unless it is possible to protect the FEA. Some of the other materials which look good in this table, can probably be discarded, due to their yield strength versus the temperature or their electrical or thermal conductivity. Also the choice of the cathode and anode should be made separately as a good cathode material might not be so well suited as an anode. The respective choices depend on the geometry of the system, and the removal of any heat generated by the dark current.

## 2.3 Electrode preparation and testing

All our electrodes tested have the same shape, see Fig.3 & 4 for the cathode and anode, respectively. The mean roughness was, by design, defined to be less than  $R_a \leq 0.2\mu\text{m}$ . In Fig.4, the copper anode, has a hole in the middle. This hole was made to mimic the behaviour of the extracting anode of the 500 kV pulser. None of the other electrodes have this hole. The  $R_a$  of the electrodes was checked after high gradient testing.

The electrodes were cleaned using acetone and alcohol in an ultra-sonic bath, before installation in the UHV system. This is the "as received" state. Unless specified otherwise none of the surfaces have been mirror finished. All materials were commercially obtained from Goodfellow<sup>TM</sup>. Technical materials refer to commercially available material, which is exposed to air before installation.

Ti and Mo electrodes were fabricated by the same machining company. Electrodes were thoroughly cleaned in acetone and alcohol before use. Ti electrodes were installed after cleaning and tested, and Mo electrodes were vacuum fired at 900°C for 3 h. After Mo testing, Ti electrodes were also vacuum fired and reused. From the literature, it was shown that heating up the material is beneficial in improving the breakdown strength [25].

The processing histories of the materials tested are summarized in Table.2. The procedure of high gradient conditioning is the same for all the cathodes. The voltage between the electrodes is applied for a given gap, 4 mm, 3 mm, 2 mm, 1.5 mm and then 1 mm.

The voltage is raised slowly, waiting for stable conditions, by discrete steps, to 60 kV and then the gap is diminished with a reduced voltage equal to the previously obtained static electrical field. It was found that above 70 kV arcing sometimes happened somewhere else in the system.

During conditioning, soft breakdowns might occur. During those breakdowns, current is measured and the pressure can increase by a factor 10. When observed, the voltage is, usually, manually reduced. The pressure recovers in a minute or two, and the voltage is again raised slowly to the previous level.

In this study, we do not reproduce quality preparation achieved in [26]. Instead, our aims were to see what is the behaviour of a technical material prepared using a less stringent procedure. Once the electrodes are installed under vacuum, our intention is to use plasma glow discharge (PGD), known to be an efficient way of cleaning surfaces and removing the contamination which can promote field emission. We do not think the exceptional surface preparation achieved by the procedure in [26] will survive an aggressive PGD.

Plasma glow discharge was usually applied after we reached 1 nA of current at 1 mm gap from the as received state. The gases injected for the PGD are usually a mixture of He and Ar, with a composition of 50% He and 50% Ar. Sometime pure Ar is used. The total pressure range was between  $\sim 0.15$  Torr and  $\sim 0.25$  Torr. Noble gases are chosen to avoid chemically attacking the surfaces. Helium is chosen because, for the same energy, its sputtering potency is less than Ar. The gases come directly from a compressed gas cylinder and are injected via a leak valve. A +400 V to +600 V bias is applied between a third electrode, Fig.2, and the two electrodes to be tested. The pressure and the energy of the ions in the PGD are adjusted, so that the plasma wraps around the electrodes. The distance between the three electrodes are around 6 cm and the time of the PGD can last between 40 to 60 minutes.

Finally, as it is known from literature that pressure can affect the breakdown onset threshold, and that dark current appearance is affected by the gas species [11], the system is baked not only after air venting but also after each plasma. By this means we minimize any role that the pressure and the gas composition would have in FE or arcing.

### 3 Results

Before presenting results obtained with our electrodes, it is of importance to bear in mind results obtained by Furuta *et al* [26, 27] and Diamond [25, 28]. According to Furuta's publication, the design of their electrodes are equivalent to ours. They have obtained, for stainless steel, Cu, Ti and Mo with mirror finished surfaces, the results summarized in Table.3. Those results have been obtained not only with mirror finished surfaces, but the assembly of their system and the mounting of their electrodes, were done in class 1 and class 10 clean room condition, respectively.

All the current vs electric field plots presented in [26] and in this work can be fitted using  $I = c E^2 e^{-a/E}$ , see Fowler-Nordheim equation (1), with I current, c and a constants, and E applied electric field. From those fits F-N parameters, area and the field enhancement  $\beta$ , can be extracted.

$$I = A \cdot \frac{1.5 \cdot 10^{-6}}{\Phi} E_s^2 \cdot e^{\frac{10.4}{\sqrt{\Phi}}} \cdot \exp\left(\frac{-6.83 \cdot 10^7 \Phi^{\frac{3}{2}}}{E_s}\right) \quad (1)$$

where  $E_s = \beta \cdot E$  and the work function, for Mo,  $\Phi$  is taken equal to 4.2 eV. However, we will not go further into the comparison between our measurements and theory, because the goal of this paper is to report on practical surface conditioning procedures to achieve stable operation under a high electric field. It is also to report on the erosion of the materials upon the field processing.

### 3.1 Aluminium Results

#### 3.1.1 Al-Al electrodes

Pristine, as received Al electrodes were tested. The first test after a thorough bake of the chamber led to a dark current of 1nA at a gap of 1 mm for a field of 7.1 MV/m. The gap between the electrodes was set at 4 mm and the electrodes were conditioned overnight by applying 29 kV and drawing 7 nA of current. The next day the dark current increased to 13 nA. Several dark current curves were then produced and compared to the as received test, Fig.5. The obvious conclusion is that our DC electrical conditioning did not lead to any improvement.

We next tested cleaning and conditioning using an He plasma of 0.26 Torr. The sputtering rate of 500 eV He ions on Al is 0.16 [6]. The 1 nA at 1 mm gap was reached for a field of 13.5 MV/m. Subsequent He plasma continued to improve the results. However, a few breakdowns occurred during the voltage processing. An ArGD at a pressure of  $\sim 0.1$  Torr produced the best results which are presented in Fig.6. The 1 nA at 1 mm gap (full circles) was reached for a field of 42 MV/m. When leaving the system at this level of field and dark current further improvement, decrease of dark current over time, is observed Fig.6 full circles. In subsequent tests, also with different materials, this improvement was occasionally observed. However, in some cases the current increased to more than the double the previous value.

In the next test an He-Ar plasma was used to clean the same electrodes. The behaviour, after pumping out the noble gases, was that no FE was observed until breakdown. The Al electrodes held stably (12hours) a field of 42 MV/m without dark current at 1.5 mm gap. Whilst the field was at 45 MV/m an arc occurred and an emission current of 350 nA could be measured. Nevertheless, damage due to this and further breakdowns during the voltage processing, were not severe; the current at 1 mm, for a field of 41.5 MV/m was still only 1 nA. Finally, the best result obtained by He-Ar GD, was a field of 52 MV/m at 1 mm without dark current. However, at some point an arc more violent than the previous ones, damaged the cathode so that no more GD was able to restore the holding of the high electric field. A summary of the performance obtained with Al electrodes is shown in Table.4.

#### 3.1.2 Mirror Finished Al Cathode

We then replaced the damaged Al cathode by a pristine mirror like finish Al (6082) cathode, machined to an  $R_a$  of 3 nm. The previously damaged mushroom anode was reused, after wiping with alcohol before reinstallation in the UHV system. The damage on the anode was localized around the summit of the anode, and resembled the right-hand picture in Fig.7.

With this configuration, the as received system held stably without dark current, up to an electric field of less than 36 MV/m. At this value, an arc occurred. Inspection of

the cathode through the viewport of the UHV system showed pitting damage. An He-Ar GD was then applied to cure and clean the electrodes. Results are summarized in Table.4. The column labelled  $<0.05$  nA shows the field strength held without measuring any FE. The system held 90 MV/m electric field at 750  $\mu$ m, and broke down at 92 MV/m. The vacuum arcing was so severe that no further PGD was able to restore such fields. Final damage to the Al electrodes is shown in Fig.7. The high field sustained shows that the breakdown is cathode initiated as the cathode was pristine and the anode was already severely damaged.

## 3.2 Copper results

Oxidized copper electrodes were tested solely after a PGD. Even after a PGD and the voltage processing, the electrodes are still very oxidized. Cleaner spots around the hole of the anode were observed at the end of the testing. Damage on the cathode was also visible. The electrodes were then cleaned by chemical etching by use of a phosphoric acid based solution Polynox<sup>®</sup>. They were subsequently rinsed with tap water and after drying, cleaned with ethanol. A last test was conducted by installing a mirror diamond turned OFHC Cu cathode ( $R_a \sim 3$  nm) and the already used Mo and then a SS anode.

### 3.2.1 Cu-Cu electrodes

The results obtained seem to show that there is no influence from the anode hole in the achievement of the high gradient, as our results are similar to what was obtained in [26], see Table.3 for clean copper.

In comparison to Al electrodes, craters in the Cu were neither as deep, nor as extended : see the 2 spots in Fig.3, compared to damages in Fig.7. All breakdown damage on the Cu anode remained localized around the hole of the mushroom. That suggests two possibilities without excluding a combination of the two. The energy in the arc was not sufficient to vaporize the Cu materials, by melting and sputtering the melted Cu, despite the fact that Cu has a higher sputtering rate than Al. Or the field was not strong enough to pull out droplets of Cu which could have then been vaporized [29].

### 3.2.2 Mirror finished Cu anode

As results from Al seemed to indicate that the breakdown is cathode initiated, a combination of a mirror finished cathode with the previously used Mo (vacuum fired ) and stainless steel(SS) anodes was tested. Those anodes had sustained damaged far less significant than the Al anode pictured in Fig.7. Results of the Cu-Mo conditioning are shown in Table.5. The conditioning of the "as received" electrode followed the "breakdown processing" or spark processing scheme, until a more severe breakdown brought the Cu anode to emit at the level of 800 nA, at 3 mm gap. During the first 500 eV ArGD, small breakdowns could be seen on the Cu cathode, which were probably dust burning away. Results obtained after plasma processing improved the situation but not to the level of the two clean Cu electrodes. It was expected that higher fields could be reached, as in the case of using two Cu electrodes, Table.5, or two Mo electrodes (see Table.6).

The Mo anode was exchanged for a SS anode, and the Cu cathode was turned 180° on its axis. Because the anode arm sags, damage on the cathode is not localized on the center of the anode, hence allowing a pristine area to be exposed. The maximum field

held with this pair was 11 MV/m at 3 mm gap, after an ArGD. From these last results, no conclusion should be drawn on the coupling of this last pair as the Cu cathode was already exhibiting an oxide color. The presence of the oxide can be due to oxygen present in the ArGD, or from oxygen being released from the Mo anode during high voltage conditioning see §3.3.5. The copper oxide is present from the center of the Cu sample to 5 mm from the sample circular edge. Microscopy and surface analysis did not reveal any material transfer from the anode (Mo or SS) to the Cu cathode.

### 3.3 Stainless steel, titanium and molybdenum results

Main results obtained, at 1 mm, for stainless steel (SS), Ti and Mo are summarized in Table.6.

#### 3.3.1 Stainless Steel

SS electrodes were electrically processed the same way as Al electrodes. After plasma treatment, the best field achieved was 68 MV/m with dark current below the 10 pA detection limit. The final breakdown, was not recoverable by the use of a PGD. Upon removal of the electrodes, damage was located at the top of the mushroom. However, craters were not as deep or as wide as for Al electrodes (in Fig.7). The damage is less extended than that observed on the Cu electrodes. If we look at the data in Table.1, this is not surprising. Effectively, both the melting point and the Young's modulus of SS are far above copper values. However, as tiny amounts of vaporized or sputtered material from the anode can be prejudicial to the working of FEAs, avoiding even soft breakdowns seems to be a good strategy.

#### 3.3.2 Titanium

In the case of Ti, we have observed after plasma treatment, a stable field holding at 52 MV/m without FE. Above 53 MV/m, dark current appeared and reached 1 nA at 62 MV/m, cf Fig.8 (diamonds). The field held at this value for a few minutes until arcing, which brought the current above 1  $\mu$ A. The field was then reduced to 35 MV/m in order to get a 1 nA current value, cf Fig.8 (squares.) This current value decreased over 56 hours of 35 MV/m field processing. A few MV/m were then gained to bring back the current to 1 nA.

It is interesting to mention that after a soft breakdown leading to dark current emission around 1  $\mu$ A, sometime no rise in pressure is detected. At a pressure of  $2.10^{-9}$  Torr, gas released by ESD process can in principle be detected. A simple calculation will show that such a current, 1  $\mu$ A, will produce a gas flux of  $\sim 3.10^{-9}$  Torr.l.s $^{-1}$ , hence an increase of pressure of  $\sim 2.10^{-11}$  Torr; assuming an ESD coefficient of  $10^{-2}$  molecule/electron. This is below the resolution of our instrumentation, and of most total pressure gauges.

A subsequent ArGD for 90 minutes at 580 eV under pressure varying from 0.156 Torr to 0.174 Torr was performed. During this PGD, the Ar gas was evacuated several times and then replaced by new Ar coming from the cylinder. The field held after this plasma was 61 MV/m. The voltage was then increased and fluctuations in the emitted current below 50 pA were observed. Between 63 MV/m and 67 MV/m the dark current was fluctuating around 0.1 nA, see Fig.9. Field conditioning over a week showed, as in the case of Al or SS, an improvement in the dark current emission. The final stable electric

field obtained for 1 nA at 1 mm gap is 55 MV/m, see insert in Fig.9. Above this level of field, the dark current does not diminish but it increases with time, Fig.9.

Upon inspection of the electrodes after their extraction from the chamber, damage spots can be seen on both electrodes. Damage is located on the anode around the top of the mushroom, and 4 separate spots can be seen on the cathode spread over a trail of 1 cm length. Damage on the Ti anode is similar to that seen on the SS and Cu anodes, in extension and morphology (melted area).

### 3.3.3 Molybdenum

Vacuum fired Mo electrodes were installed in the system, the best results are summarized in Table.6. A simple 25Hz optical camera was used to view the electrodes, hence the space in between. When running, no light is present in the system enclosure. During the soft events, a flash is seen on the TV screen and a jump in current intensity, below 0.1 nA, is measured sometimes associated with a pressure increase. The flash is localized and takes the full space occupied between the electrodes. During harder breakdowns, sound can be heard coming from the enclosure. After these soft breakdowns, the voltage could still be increased. In order to have a chance to detect breakdown precursor, fast acquisition and very high sensitivity, to single photon, are mandatory. However, such a simple optical system can be used as an interlock protection for our FEL.

As for the Ti electrodes, dark current appears at some voltage, contrary to Al, Cu and SS electrodes where dark current appears only after a breakdown. Raising the field further increased the dark current until breakdown occurred. Dark current plots from as received electrodes(triangles), and after three plasma treatments are presented in Fig.10. The first ArGD pushed the limits of the dark current onset (diamonds) until a hard breakdown occurred, bringing the current into the  $\mu$ A range. The onset and the 1 nA limit was then greatly reduced (squares). The second ArGD enabled partial recuperation from this breakdown (asterisks). A third plasma He-Ar, did not bring any extra improvement (crosses in squares). Mo conditioning from broad electrodes at large gap ( $> 500\mu\text{m}$ ) was similar to conditioning with short gaps. Mo reached a higher gradient than Cu but it sparked more to get there [24], hence showing more damage than Cu, Fig.3. From this, it is obvious that a special electrode conditioning procedure must be used to process the Mo electrodes, and thus to protect the electron source (FEA).

### 3.3.4 Titanium vacuum fired

Original Ti electrodes were re-installed after vacuum firing and the results, for comparison with non fired Ti, are presented in Table.6. After vacuum firing the Ti became gray black. This color can indicate  $\text{TiH}_2$  or  $\text{TiO}_2$  in the rutile form, or  $\text{Ti}_3\text{O}_5$ . Damage, all localized on the top of Ti anode, can be seen in Fig.4. The involuntary coating is removed by the severe breakdowns sustained by both electrodes.

### 3.3.5 Surface analysis

Given the rather poor performances in field holding for the Mo electrodes, compared to literature values, and the colour of the Ti electrodes, it is suspected that the vacuum firing degraded the Mo properties instead of improving them. The pressure in the vacuum furnace was probably around  $10^{-5}$  Torr. Ti and Mo cathodes were sent for surface analysis, X-ray photoelectron (XPS) and Auger (AES) spectroscopy. Upon AES analysis, the

surfaces of both electrodes exhibited high contents of carbon (C) and oxygen (O), higher than normal air exposure. Nitrogen (N) is also present on the Mo surface. Nitrogen cannot be seen on Ti as Ti and N overlap under AES analysis. Under XPS analysis, a shift of about 5 eV to higher binding energy, for both Mo 3d<sub>5/2</sub> and Ti 2p<sub>3/2</sub> is observed. Such shift can be the mark of TiO<sub>2</sub> and MoO<sub>3</sub> [30]. The Mo shows no discoloration, suggesting the formation of a thin trioxide film. The conclusions are, first of all a small air leak might have been present in the furnace. Secondly, a bad heat treatment will bring the opposite results in terms of field holding.

## 4 Conclusions

Plasma glow discharge is a very effective way to enhance the DC field holding in between two broad electrodes. It also permits restoration and sometimes improvement of the DC field limit achieved after a breakdown event leading to dark current emission. This dark current follows the FN law.

The downside of such treatment, for Al, Cu and SS electrodes, is that the surfaces hold the field until breakdown with no or little warning. No increase in pressure is recorded, but sometime some current variation in the tens of pA might appear. Such fluctuations can be the sign of a forthcoming breakdown, if any, but the time scale can vary from minutes to hours. In the hunt for the breakdown precursor, in the framework of an interlock for the 500 kV pulser, a highly sensitive and fast photomultiplier will be tested in this 100 kV DC test stand.

For Ti and Mo electrodes dark current appears and increases when raising the voltage until breakdown occurs. However, during the processing a few sparks occur, sometimes in a "spitfest" regime. Those sparks are beneficial as they condition the surface. Dark current at a level of 1 nA can either drift to hundreds of nA, fall back to less than a hundred pA or stay stable. So far, the prediction for its evolution is only empirical.

Finally we have, without stringent procedures, matched or exceeded results obtained by other labs. However, results for non mirror finished Ti and Mo were below the ones obtained elsewhere. In the case of Mo, it is suspected that the vacuum firing contaminated the Mo as it did for Ti, leading to poorer performances than usually reported in the literature.

In order to find the Grail material, which will hold our requested field without emitting dark current, Niobium seems to be a material of interest. Ion implantation, with nitrogen, is known to harden materials [31, 32]. It may be possible that this technique of hardening can be useful to increase the breakdown threshold of soft materials, as it seems to have for harder ones [33]. Dark current from electrodes can be lowered by depositing a pure monolayer of oxygen on the surface, which will increase the work function of the electrodes. However, and in the framework of an accelerator electron source, this layer might have to be regenerated frequently as back bombardement from residual gas ions will clean the surface.

## 5 Acknowledgments

Kugler GMBH for the donation of the mirror finished Al and Cu cathodes. R. Kirby (SLAC) and U. Mueller (EMPA Duebendorf) for the surface analysis. S. Ritter (PSI) for

the SEM time. Finally, to M. Taborelli, T. Ramsvik, S. Sgobba at CERN and E. Kirk (PSI) for some useful discussion.

## References

- [1] R. Bakker. LEG Project Overview. In *First annual EUROFEL workshop, Orsay/Saclay, France*, 2005.
- [2] A.E Candel. *Simulation of Electron Source for Next-Generation X-ray Free-Electron Laser*. PhD thesis, Ecole Polytechnique Fédérale Zürich, 2005. ETHZ-IPP 2005-11.
- [3] M. Paraliev, C. Gough, S. Ivkovic. Tesla coil design for electron gun application . In *15<sup>th</sup> IEEE International Pulsed Power Conference, Monterey, USA*, 2005.
- [4] P.A Redhead. The First 50 Years of Electron Stimulated Desorption (1918-1968). *Vacuum*, 48 (6):585, 1997.
- [5] R.D. Ramsier and J.T. Yates Jr. Electron-Stimulated Desorption: Principles and Applications. *Surface Science Reports*, 12 (6-8):243, 1991.
- [6] J.L. Vossen, W. Kern. *Thin Film processes*. Academic Press, 1978.
- [7] S. Cernusca. *Electron Emission and Nanodefects due to Slow Ion Impact on Solid Surfaces*. PhD thesis, Technischen Universität Wien, 2003.
- [8] I.C. Gebeshuber, S. Cernusca, F. Aumayr, HP. Winter. AFM search for slow MCI-produced nanodefects on atomically clean monocrystalline insulator surfaces. *Nuclear Instruments and Methods in Physics Research B*, 205:751, 2003.
- [9] R. Dei-Cas. Review of High - brightness Electron Guns. In *EPAC, Berlin, Germany*, 1992.
- [10] J. Grames et al. Lifetime Measurements using the JLAB load-lock Gun. In *PESP, Mainz, Germany*, 2004.
- [11] L.L Laurent. *High Gradient RF Breakdown Studies*. PhD thesis, University of California Davis, 2002.
- [12] G.R. Werner. *Probing and Modeling Voltage Breakdown in Vacuum*. PhD thesis, Cornell University, 2004.
- [13] D.M. Goebel. High Voltage Breakdown Limits of Molybdenum and Carbon-based Grids for Ion Thrusters. In *41<sup>st</sup> AIAA/ASME/SAE/ASEE Joint Propulsion Conference & Exhibit*, 2005. AIAA 2005-4257.
- [14] R.J. Noer. Electron Field Emission from Broad-Area Electrodes. *Applied Physics A*, 28:1–24, 1982.
- [15] S. Kobayashi, H. Kojima, Y. Saito. Influence of in-situ ion beam sputter cleaning on the conditioning effect of vacuum gaps. In *SPIE - Discharges and Electrical Insulation in Vacuum*, volume 2259, page 364, 1994.

- [16] S. Kobayashi. Recent Experiments on Vacuum Breakdown of Oxygen-Free Copper Electrodes. *IEEE Trans. DEI*, 4:841, 1997.
- [17] R. Calder, A. Grillot, F. Le Normand and A.G Mathewson. Cleaning and Surface Analysis of Stainless Steel Ultrahigh Vacuum Chambers by Argon Glow Discharge. In *Proc. of the 7<sup>th</sup> Int. Vac. Congress*, 1977. IVC & ICSS Vienna, Austria.
- [18] David R. Lide, editor. *Handbook of Chemistry and Physics*. 74<sup>th</sup> edition. CRC PRESS, 1994.
- [19] W.M. Posadowski, Z.J. Radzimski. Sustained self-sputtering using a direct current magnetron source. *Journal of Vacuum Science and Technology*, A11(6), 1993.
- [20] A. Anders et al. Self-Sustained Self-Sputterinng: A Possible Mechanism for the Superdense Glow Phase of a Peudopark. *IEEE Transactions on Plasma Science*, 23 (3):275, 1995.
- [21] R.S. Mason and M. Pichilingi. Sputtering in a glow discharge ion source - pressure dependence: theory and experiment. *J. Phys. D :Appl Phys*, 27:2363, 1994.
- [22] V. Dolgashev and S.G. Tantawi. RF breakdown in X-band Waveguides. In *EPAC 2002, France*, 2002. SLAC-PUB-10355.
- [23] D.W. Williams and W.T. Williams. Effect of electrode surface finish on electrical breakdown in vacuum. *J. Phys.D:Appl.Phys*, 5:1845, 1972.
- [24] M. Kildemo, S. Calatroni, M. Taborelli. Breakdown and Field Emission Conditioning of Cu, Mo and W. *Phys. Rev. Special Topics - Accelerators and Beams*, 7, 2004.
- [25] W.T Diamond. New perspectives in vacuum high voltage insulation. I. The transition to field emission. *Journal of Vacuum Science and Technology*, A16(2), 1998.
- [26] F. Furuta et al. Reduction of Field Emission Dark Current for High-Field Gradient Electron Gun by Using a Molybdenum Cathode and Titanium Anode. *Nuclear Instruments and Methods in Physics Research A*, 538:33–44, 2005.
- [27] C. Suzuki et al. Fabrication of ultra-clean copper surface to minimize field emission dark currents. *Nuclear Instruments and Methods in Physics Research A*, 462:337, 2001.
- [28] W.T Diamond. New perspectives in vacuum high voltage insulation. II. Gas desorption. *Journal of Vacuum Science and Technology*, A16(2), 1998.
- [29] G.A. Mesyats and S.A. Barenholz. The "Hunting Effect" in the cathode region of a vacuum arc. In *ICPIG 2003, Germany*, 2003.
- [30] *Handbook of X-Ray Photoelectron Spectroscopy*. Perkin-Elmer Corporation, 1992.
- [31] E. Woolley. Hardness goes skin-deep. *Materials World*,, 5(10):515, 1997. <http://www.azom.com/details.asp?ArticleID=552>.
- [32] A. Shokouhy et al. Surface modification of AISI 304 Stainless Steel using nitrogen ion implantation. In *ICPIG 2005, Holland*, 2005.

[33] C.K. Sinclair et al. Dramatic Reduction of DC Field Emission from Large Area Electrodes by Plasma-Source Ion Implantation. In *PAC, Chicago, USA*, 2001.

Table 1: Secondary electron yield maximum [18], sputtering yield by 500 eV incident Ar [6] and self-sputtering rate at 500 eV of different elements [19, 20].

Elements	SEYmax	Atm/Ar inc	Self Sputter rate	Melting Point °C	Young Modulus GPa
Cu	1.3	2.3	> 1	1083	110
Al	1.0	1.05	< 1	660	69
Au	1.4	2.4	> 1	1063	78
Ti	0.9	0.5	< 1	1668	116
Mo	1.25	0.6	< 1	2610	329
Zr	1.1	0.65	< 1	1852	68
Fe	1.3	1 (SS 1.3)	~ 1 [21]	1536	200
W	1.4	0.57	< 1	3410	411
Ta	1.3	0.57	< 1	2996	186
Nb	1.2	0.6	< 1	2415	105

Table 2: Measurement history of air-exposed dark current electrodes.

Cathode	Anode	As received	Plasma (He - Ar)	n <sup>th</sup> Plasma
SS	SS	Yes	Yes	Yes
Al	Al	Yes	Yes	Yes
Al mirror Finished	Al (sme as abv)	Yes	Yes	Yes
Cu oxidized	Cu oxidized	-	Yes	Yes
Cu Polynox™	Cu Polynox™	Yes	Yes	-
Ti	Ti	Yes	Yes	Yes
Mo vac fired	Mo vac fired	Yes	Solely Ar	Yes
Ti vac fired	Ti vac fired	Yes	Solely Ar	Yes
Cu mirror Finished	Mo vac fired	Yes	Solely Ar	Yes

Table 3: Field gradient (MV/m) between electrodes obtained at 1 mm gap for 1 nA of dark current or with no field emission (FE), second row.

	SUS	Cu	Ti	Mo	Mo - Ti	Al	Nb
1 nA [26]	36	47.5	88	84	103	-	-
No FE [25]	-	70	60	-	-	85	92

Table 4: Electric field in MV/m held in between two Al electrodes at 1 mm gap for the given dark current in nA.

	Al - Al		Al mirror finished - Al	
State / Dark Current	< 0.05 nA	1 nA	< 0.05 nA	1 nA
As Received	-	7.5	36 (2 mm)	29
After Plasma	52	30	73 (stable) (92 at 750 $\mu$ m)	31

Table 5: Electric field in MV/m held in between Cu electrodes at 1 mm gap for the given dark current in nA. (\*) obtained at 3mm gap

	Cu oxidized		Cu clean		Cu-Mo	
State / Dark Current	< 0.05 nA	1 nA	< 0.05 nA	1 nA	< 0.05 nA	1 nA
As Received	-	-	24	26	18.2 (*)	13.8 (*)
After Plasma	32	29.3	55	19	21.6	25.4

Table 6: Electric field in MV/m held in between two SS two Ti and two Mo electrodes at 1 mm gap for the given dark current in nA.

	State / Dark Current	< 0.05 nA	1 nA
SS	As Received	40	42.5
	After Plasma	68	35
Ti	As Received	50	46.6
	After Plasma	63	67 (0.1nA)
Ti Vac Fired	As Received	29.6	32.5
	After Plasma	39	41.4
Mo Vac Fired	As Received	37	45.2
	After Plasma	44	61.3

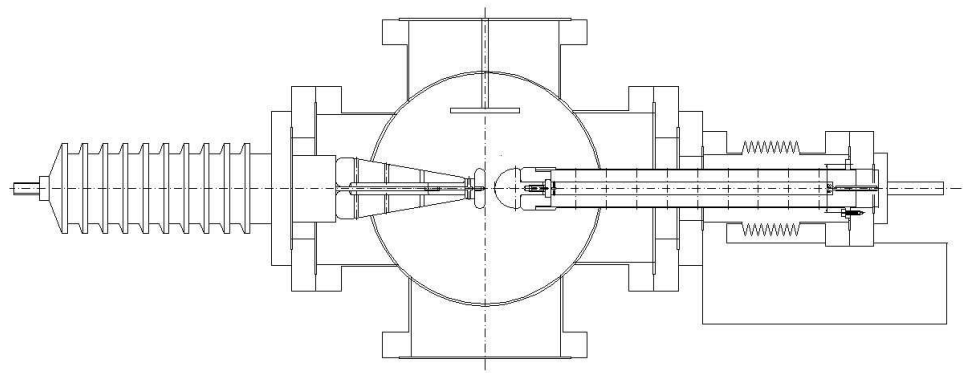


Figure 1: Dark Current -100 kV DC test stand.

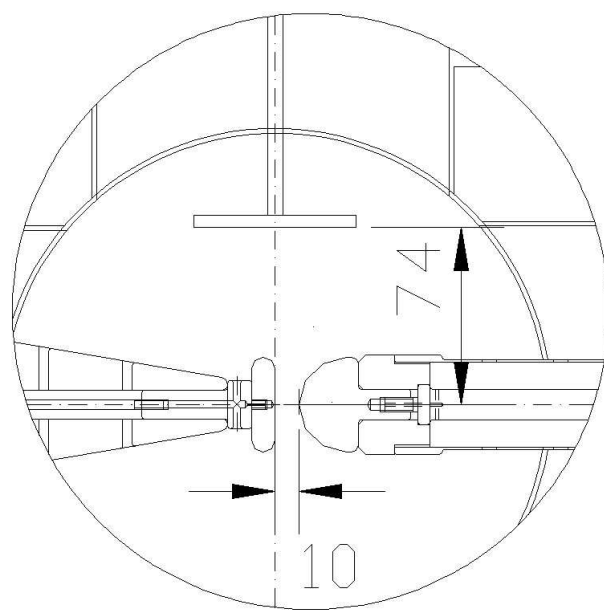


Figure 2: Dark Current -100 kV DC test stand. Zoom over the area containing the cathode (flat electrode) the anode (mushroom) and the plasma electrode located at 7 cm from the center of the system

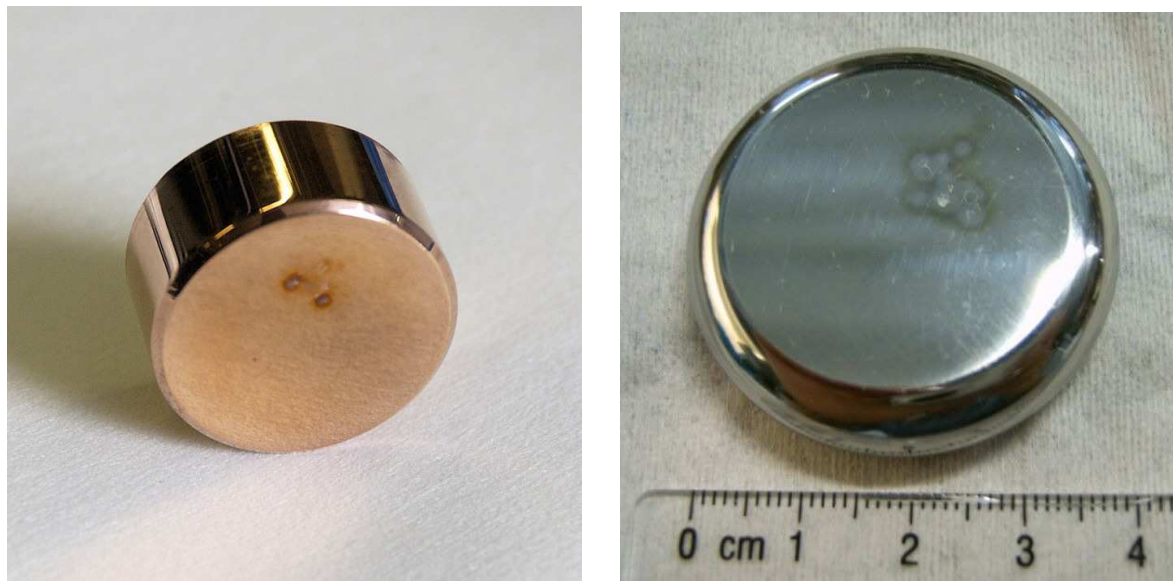
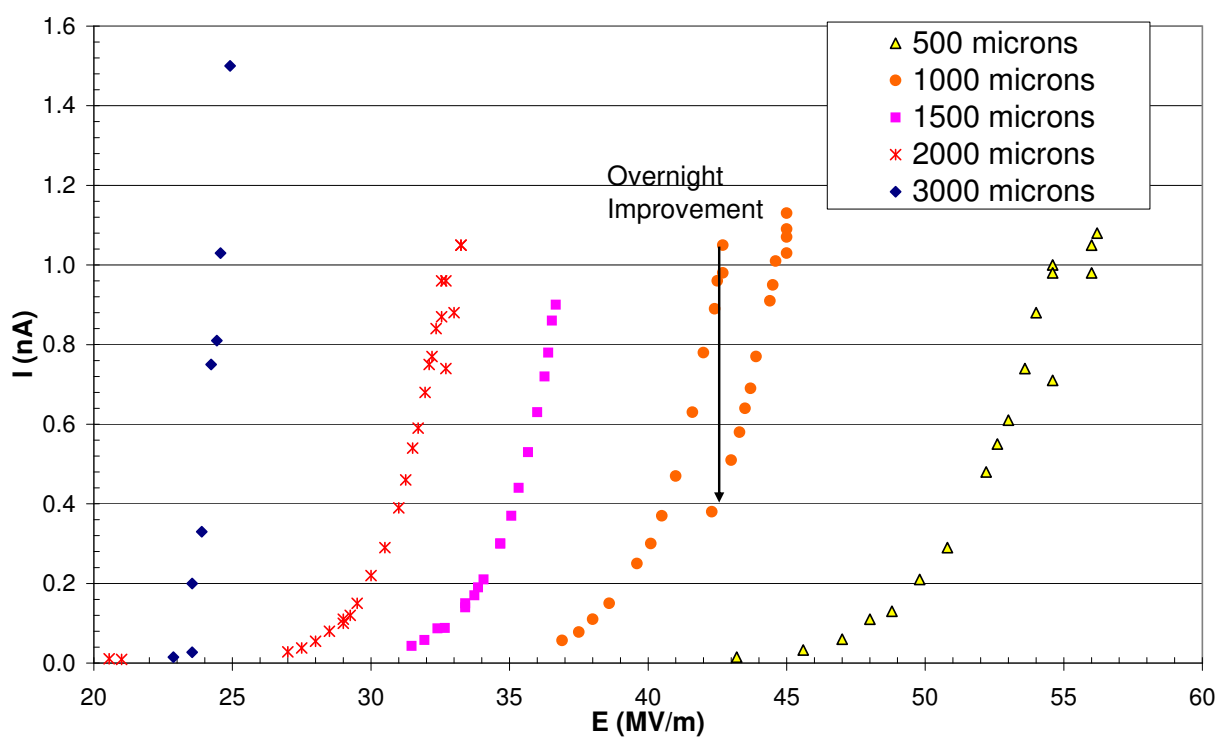
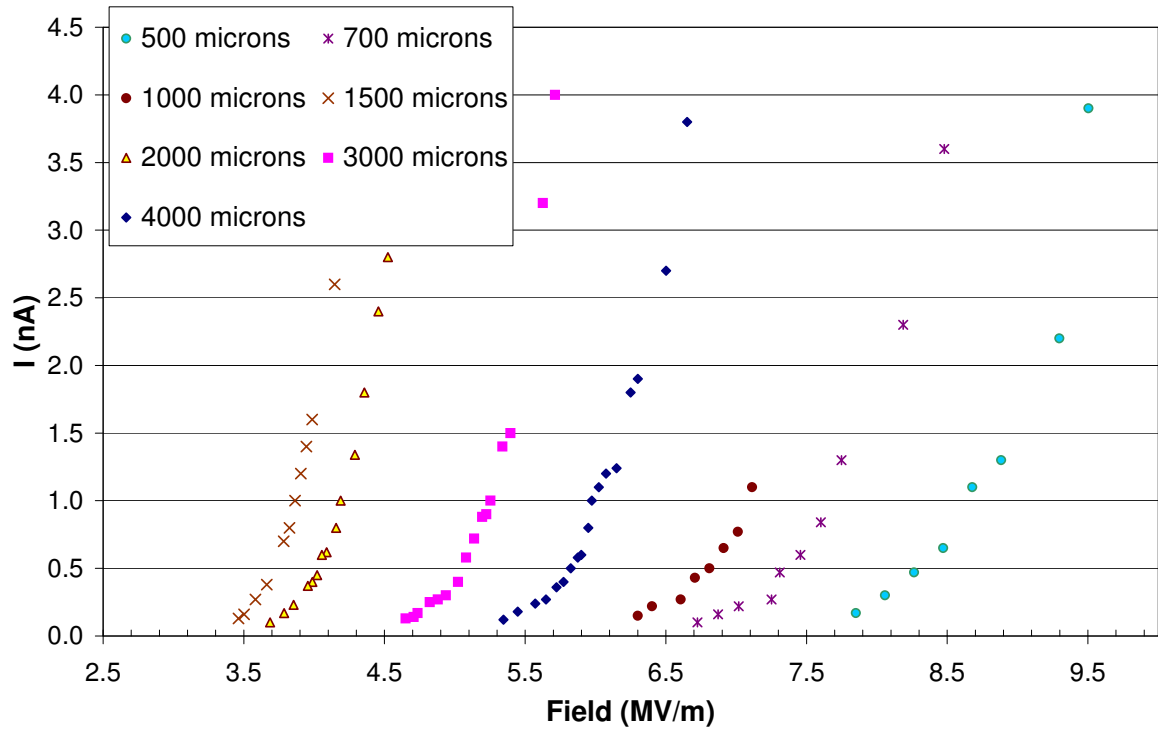


Figure 3: Cleaned Cu cathode after high voltage testing, left. Damaged Mo cathode, right picture. Damage can be clearly seen.



Figure 4: Three anodes used for HV testing, Ti on the left(grey black colour, after vacuum firing), Mo in the center and Cu on the right. Pictures taken after HV testing. Damage can be seen on the Ti electrodes



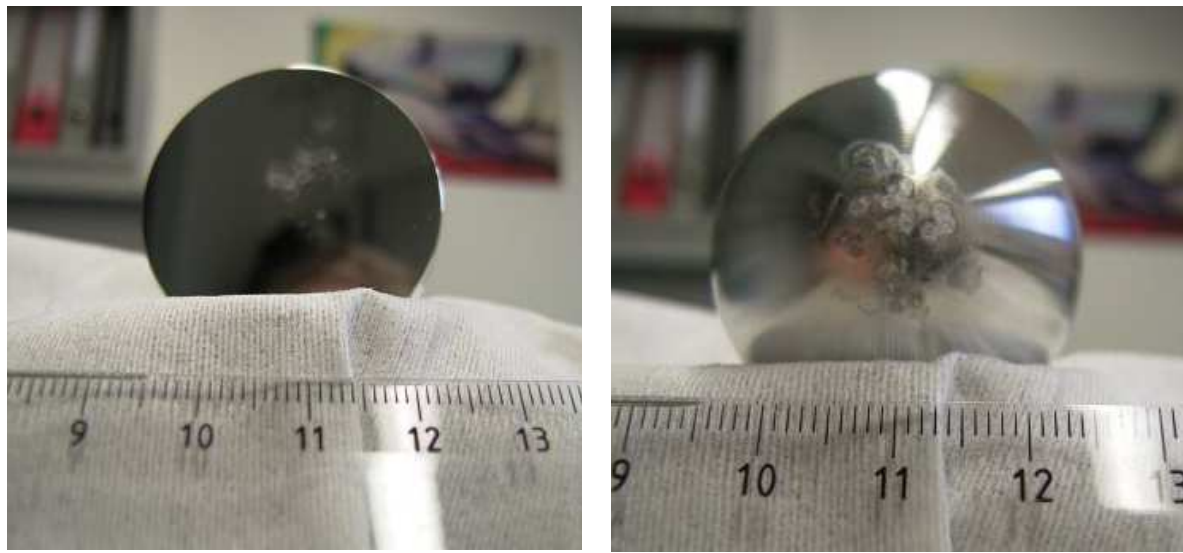


Figure 7: Breakdown damage withstood by the Al cathode (mirror finished-left) and anode (right) during the conditioning period. Scale in cm.

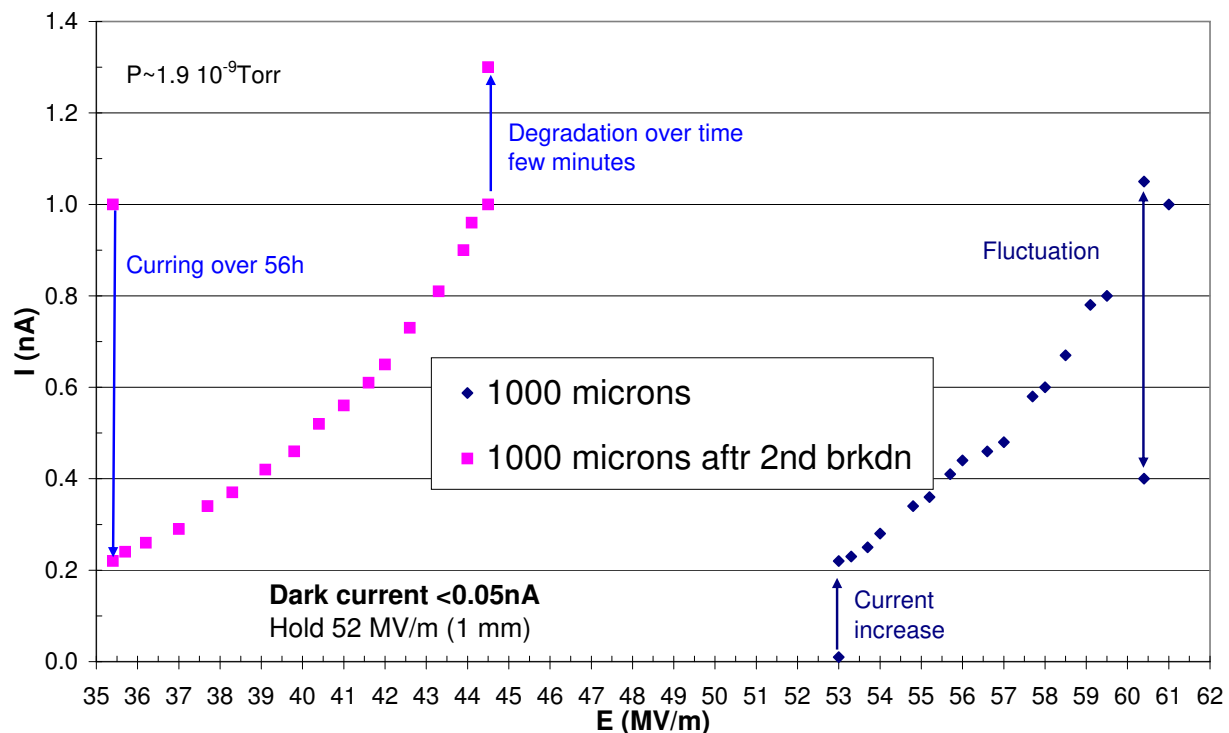


Figure 8: Dark current evolution of Ti electrodes after a 2<sup>nd</sup> Ar Glow Discharge. The square curve is obtained after a surface breakdown at 62 MV/m

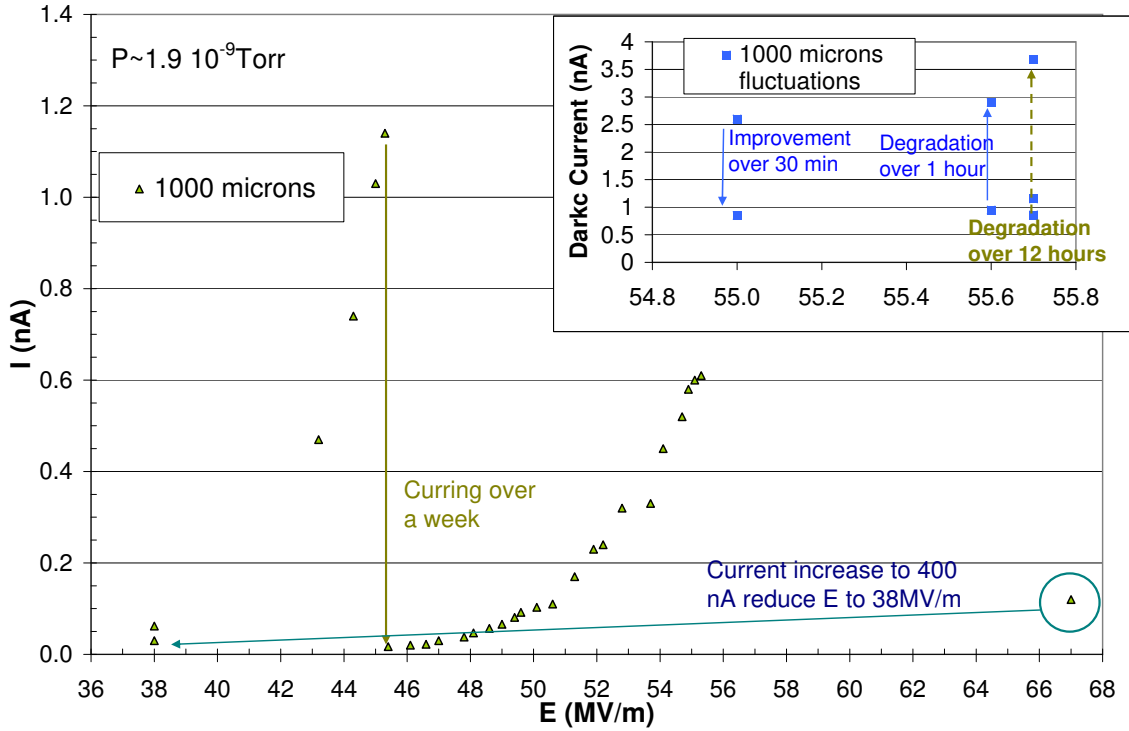


Figure 9: Dark current evolution of Ti electrodes after a 3<sup>rd</sup> Ar Glow Discharge.

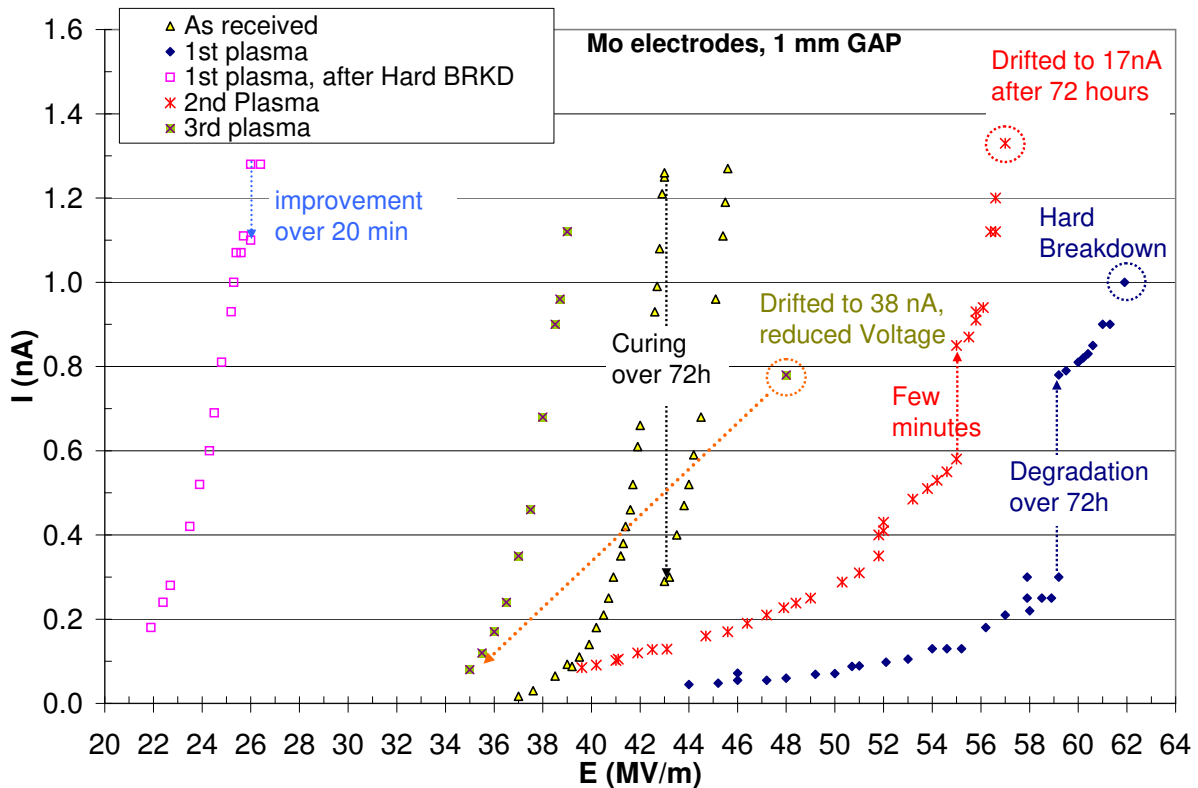


Figure 10: Dark current evolution of Mo electrodes after processing.

## List of Tables

1	Secondary electron yield maximum [18], sputtering yield by 500 eV incident Ar [6] and self-sputtering rate at 500 eV of different elements [19, 20]. . . . .	13
2	Measurement history of air-exposed dark current electrodes. . . . .	13
3	Field gradient (MV/m) between electrodes obtained at 1 mm gap for 1 nA of dark current or with no field emission (FE), second row. . . . .	14
4	Electric field in MV/m held in between two Al electrodes at 1 mm gap for the given dark current in nA. . . . .	14
5	Electric field in MV/m held in between Cu electrodes at 1 mm gap for the given dark current in nA. (*) obtained at 3mm gap . . . . .	14
6	Electric field in MV/m held in between two SS two Ti and two Mo electrodes at 1 mm gap for the given dark current in nA. . . . .	14

## List of Figures

1	Dark Current -100 kV DC test stand. . . . .	15
2	Dark Current -100 kV DC test stand. Zoom over the area containing the cathode (flat electrode) the anode (mushroom) and the plasma electrode located at 7 cm from the center of the system . . . . .	16
3	Cleaned Cu cathode after high voltage testing, left. Damaged Mo cathode, right picture. Damage can be clearly seen. . . . .	17
4	Three anodes used for HV testing, Ti on the left(grey black colour, after vacuum firing), Mo in the center and Cu on the right. Pictures taken after HV testing. Damage can be seen on the Ti electrodes . . . . .	17
5	Dark current of Al electrodes after a system bake at 190°C for 100h and after electrical conditioning of 29 kV at a 4 mm gap drawing 7 nA of current from the cathode to the anode. . . . .	18
6	Dark current of Al electrodes after an Ar Glow Discharge, following the previous He processing and high field conditioning. . . . .	18
7	Breakdown damage withstood by the Al cathode (mirror finished-left) and anode (right) during the conditioning period. Scale in cm. . . . .	19
8	Dark current evolution of Ti electrodes after a 2 <sup>nd</sup> Ar Glow Discharge. The square curve is obtained after a surface breakdown at 62 MV/m . . . . .	19
9	Dark current evolution of Ti electrodes after a 3 <sup>rd</sup> Ar Glow Discharge. . . . .	20
10	Dark current evolution of Mo electrodes after processing. . . . .	20